Asymmetric inheritance of centrosomes maintains stem cell properties in human neural progenitor cells

Lars N. Royall[1], Annina Denoth-Lippuner[1], Sebastian Jessberger[1*]

[1]Laboratory of Neural Plasticity, Faculties of Medicine and Science, Brain Research Institute, University of Zurich, 8057 Zurich, Switzerland. [*]Correspondence should be addressed to S.J. (jessberger@hifo.uzh.ch)

Impact Statement

Genetic birthdating in forebrain organoids shows asymmetric inheritance of centrosomes in human neural progenitor cells, required for proper human neurogenesis.

Keywords

Neurogenesis, centrosome, asymmetric cell division, organoid, human neural progenitor cell

Abstract

During human forebrain development, neural progenitor cells (NPCs) in the ventricular zone (VZ) undergo asymmetric cell divisions to produce a self-renewed progenitor cell, maintaining the potential to go through additional rounds of cell divisions, and differentiating daughter cells, populating the developing cortex. Previous work in the embryonic rodent brain suggested that the preferential inheritance of the pre-existing (older) centrosome to the self-renewed progenitor cell is required to maintain stem cell properties, ensuring proper neurogenesis. If asymmetric segregation of centrosomes occurs in NPCs of the developing human brain, which depends on unique molecular regulators and species-specific cellular composition, remains unknown. Using a novel, recombination-induced tag exchange (RITE)-based genetic tool to birthdate and track the segregation of centrosomes over multiple cell divisions in human embryonic stem cell (hESC)-derived regionalized forebrain organoids, we show the preferential inheritance of the older mother centrosome towards self-renewed NPCs. Aberration of asymmetric segregation of centrosomes by genetic manipulation of the centrosomal, microtubule-associated protein Ninein alters fate decisions of NPCs and their maintenance in the VZ of human cortical organoids. Thus, the data described here use a novel genetic approach to birthdate centrosomes in human cells and identify asymmetric inheritance of centrosomes as a mechanism to maintain self-renewal properties and to ensure proper neurogenesis in human NPCs.

Introduction

During human brain development, neural progenitor cells (NPCs) undergo two modes of cell division. At first, NPCs, at this developmental stage called neuroepithelial cells, undergo expansive symmetric divisions (Cadwell et al., 2019; Libe-Philippot and Vanderhaeghen, 2021). Symmetric divisions are characterised by the generation of two daughter cells of similar fate; here, two NPCs both retain their potency, their capacity to self-renew and remain in the ventricular zone (VZ). Around gestational week (GW) 5 in the developing human brain (corresponding approximately to embryonic day (E) 11.5 in the mouse embryo), NPCs, at this developmental stage referred to as radial glia or apical progenitor cells, transition from an expansive phase into a neurogenic phase and shift their mode of division from symmetric to asymmetric divisions (Cadwell et al., 2019; Libe-Philippot and Vanderhaeghen, 2021). Asymmetric divisions result in two daughter cells with different fates and cellular behaviour: one daughter remains in the VZ and retains the ability to self-renew, comparable to the mother cell. The other daughter cell migrates along the basal process of their sister cell, out of the VZ and either directly begins the process of neuronal differentiation or initiates additional rounds of symmetric, differentiating cell divisions producing two neurons (at this stage referred to as intermediate progenitors or basal progenitor cells) (Noctor et al., 2004; Hansen et al., 2010; Gao et al., 2014). Exactly how differential fates of sister cells are established remains not completely elucidated; however, previous work showed that the centrosome might play a central role in distinct fates of daughter cells upon neurogenic, asymmetric cell divisions (Wang et al., 2009).

Centrosomes are unbound organelles comprised of two centrioles connected by a flexible linker and surrounded by a dynamic protein matrix called pericentriolar

material. Centrosomes are the primary microtubule organising centres of metazoan cells and provide the contractile forces required for mitosis in most human cells (Bornens, 2002). The centrosome duplicates once per cell cycle that occurs in a semi-conservative way, producing one centrosome that is older and functionally more mature than the other one. At mitosis, the older and younger centrosome will always be asymmetrically segregated to one of the two daughter cells. Previous work showed that there is non-random inheritance of centrosomes based on their age in the developing cortex of flies (Januschke et al., 2011; Ranjan et al., 2019; Sunchu and Cabernard, 2020), chickens (Tozer et al., 2017) and mice (Wang et al., 2009; Paridaen et al., 2013). Indeed, in the mouse developing cortex self-renewing NPCs appear to inherit the older, more mature centrosome while the newborn neuron inherits the new, daughter centrosome (Wang et al., 2009). Notably, randomization of centrosome inheritance leads to premature depletion of NPCs from the VZ, indicating functional relevance of asymmetric centrosome inheritance during mouse cortical development (Wang et al., 2009). How asymmetric centrosome inheritance affects cellular fate is only poorly understood but, for example, recent work showed that Mind-bomb1, a Notch signalling regulator, is preferentially enriched at the younger centrosome, asymmetrically segregates with it into the differentiating daughter cell, and thereby potentially promotes stemness via Notch signalling activation in surrounding NPCs (Tozer et al., 2017).

Despite substantial evidence supporting the importance of asymmetric centrosome inheritance in NPCs from diverse, evolutionary distant species, there is little known about human tissues. This is mainly due to the difficulty obtaining samples of human developing cortex coupled with the fact that asymmetric divisions are rarely, if not ever, seen *in vitro* in 2-dimensional (2D) cell cultures. However, it is

clear that the human gyrencephalic brain relies on species-specific molecular regulators and shows a substantially distinct cellular composition compared to the lissencephalic rodent brain. For example, the human developing brain harbours asymmetrically dividing NPCs in the outer subventricular zone, referred to as basal radial glia, which are rare in the developing cortex of lissencephalic animals (Hansen et al., 2010; Ostrem et al., 2017; Llinares-Benadero and Borrell, 2019). Recent methodological advances such as the generation of brain organoids, derived from human pluripotent stem cells, recapitulate early steps of human brain development, allowing for novel approaches to characterize the principles of cortical development in human tissues (Lancaster et al., 2013; Di Lullo and Kriegstein, 2017). Here, we used human embryonic stem cell (hESC)-derived, regionalized forebrain organoids as a model of early human cortical development to identify the dynamics and functional relevance of asymmetric centrosome inheritance for human neurogenesis.

Results

Centriolin-RITE birthdates human centrosomes

With the aim to birthdate and track the segregation of centrosomes over multiple cell divisions in human cells we created a novel genetic tool based on the recombination-induced tag exchange (RITE) system (Hotz et al., 2012), consisting of the red fluorescent protein tdTomato flanked by LoxP sites and followed by a second section containing the green fluorescent protein NeonGreen (with each section ending with a terminal stop codon followed by a 3'UTR or a T2A Neo respectively) (Figure 1A). Using CRISPR/Cas9 (Ran et al., 2013) we inserted the RITE construct into hESCs immediately upstream of the terminal stop codon of Centriolin, a protein that localises to the subdistal appendages of the mother centriole (Gromley et al., 2003; Gromley et al., 2005; Kashihara et al., 2019; Chong et al., 2020). The Centriolin yeast ortholog, Nud1, has previously been shown to have limited turnover on the pre-existing yeast spindle pole body (Lengefeld et al., 2017). As the reading frame is maintained, Centriolin will be constitutively tagged with tdTomato. LoxP recombination with Cre recombinase will excise the first section containing tdTomato, causing Centriolin to be tagged with NeonGreen, and allowing for the discrimination of pre-existing vs. newly synthesized Centriolin based on red vs. green fluorescence. Indeed, tdTomato positive dots were observed in each cell and NeonGreen was detectable within 24 hours after recombination induced by electroporation of Cre recombinase expressing plasmid; staining with the centrosomal marker protein Pericentrin showed that Centriolin-tdTomato was properly localising to the centrosome (Figure 1B). Correct localization of RITE-tagged Centriolin was confirmed by live imaging of hESCs following electroporation of GFP-Centrin-1, which localised to the centrioles (Supplementary Figure 1A). In line with the known

behaviour of Centriolin as a subdistal appendage of the mother centriole, Centriolin-tdTomato co-localised to one of the two centrioles.

Examination of cells at different stages of mitosis showed that Centriolin-tdTomato signal was present in prophase cells but diminished by metaphase (Figure 1C). To investigate whether this was due to loss of Centriolin-tdTomato protein or quenching of fluorescence, we stained for tdTomato, which revealed that Centriolin-tdTomato protein remained localised to the centrosome throughout mitosis (Figure 1D), indicating that RITE-tagged Centriolin allows for tracking centrosomes in human cells. To simplify and facilitate Cre recombinase-mediated recombination without the need of transfection or electroporation we used CRISPR/Cas9 to introduce a stable expression cassette of ER^{T2}-CRE-ER^{T2} from the human *safe harbour* locus Adeno-associated virus site 1 (AAVS1; Roemer, 2016), which we used for subsequent experiments.

Centriolin-RITE localisation and recombination in human forebrain organoids

We used a heterozygous Centriolin-RITE, ER^{T2}-CRE-ER^{T2} positive hESC line to generate regionalized, forebrain organoids (Supplementary Figure 1B) to understand how centriolin localises within the 3-dimensional structure of human neural tissues (Qian et al., 2016; Denoth-Lippuner et al., 2021). Day 35 organoids were fixed and stained with the centrosomal marker CEP164 to check for correct colocalization of RITE-tagged Centriolin within organoids. Indeed, CEP164 co-staining confirmed co-localization with Centriolin-tdTomato (Figure 2A). Ventricle-like structures at the center of cortical units were easily identifiable by the clustering of Centriolin-

tdTomato-labeled centrosomes, belonging to SOX2-positive, NPCs in the VZ (Figure 2A). Centrosomes outside of the VZ were more sparsely distributed.

To test whether Centriolin-RITE organoids maintain their capacity to recombine, day 35 organoids were incubated with 4-OH tamoxifen to induce nuclear translocation of the ER^{T2}-Cre-ER^{T2} and thus the recombination of the LoxP sites in the RITE system. Presence of Centriolin-NeonGreen was detected both inside and outside the ventricle, indicating successful recombination (Figure 2B). Interestingly, we observed centrosomes with varying NeonGreen-to-tdTomato ratios, indicating centrosomes of varied ages. Such mixed tdTomato and NeonGreen centrosomes were observed at longer time points (>20 days) after recombination indicating that centriolin was remarkably stable on the centrosome, labeled with CEP164.

Ventricular NPCs retain the older centrosome

To assess whether there is an asymmetric inheritance of older centrosomes, the RITE-tagged centrosome signal was compared between NPCs in the VZ and progeny that had migrated away from the center of cortical units. NPCs in VZ were selected for comparison, as opposed to all SOX2-positive cells, as their presence in the VZ strongly indicates their capacity for self-renewal whereas SOX2-positive cells outside of the VZ may have already started differentiation along the neural lineage.

Twenty-two days after recombination organoids were stained and the ventricles, and the surrounding tissue, were imaged (Figure 2C). During this process, the 3-D tissue gets collapsed into a 2-D image. As ventricle-like structures in organoids are tubular or spherical in nature, this dimension collapse produces a circle of centrosomes, where multiple Z planes show a ring (Figure 2D and

Supplementary Figure 1C). This leads to an inclusion of centrosomes whose cell bodies are not imaged because of the radial orientation of NPCs relative to the ventricles and the volume of tissue imaged. This is problematic as the progeny of the recombined NPCs whose centrosomes are on the inner ventricular wall (shown in purple in Figure 2D) would migrate along the NPCs' radial projection and would not be in the imaged area. However, NPCs whose centrosomes are on the outer ventricular wall will produce progeny that should remain in the imaged area (shown in orange and yellow in Figure 2D). The inclusion of NPC centrosomes and not their progeny could potentially skew the data. To correct for this, images were digitally subdivided into areas of recombined NPCs and their likely progeny (Figure 2E). Centrosomes were manually allocated a colour by the quantity of Centriolin-tdTomato signal present in recombined centrosomes. Orange centrosomes' tdTomato signals were visibly indistinguishable from non-recombined centrosomes (Figure 2F); yellow centrosomes had some tdTomato signal but less compared to non-recombined centrosomes and green centrosomes showed no detectable tdTomato signal. The number of orange, yellow and green centrosomes were counted in the VZ section (vent) and the non-VZ section (nonvent) and compared. Comparison between these two regions revealed a higher proportion of orange centrosomes in the ventricle compared to outside the ventricle (Figure 2G-H, Supplementary Table 1). The inverse was observed for green centrosomes, whereas there was no difference seen in the localisation of yellow centrosomes, similar to what was observed in the absolute number of each centrosome colour (Figure 2H). To validate the manual approach, we used an unbiased method of analysing fluorescence levels at the centrosomes. The mean tdTomato and NeonGreen signal was acquired, and a ratio was calculated for each centrosome (see Methods for

details). This analysis showed that VZ centrosomes had a lower proportion of NeonGreen signal compared to their non-ventricular progeny (Supplementary Figure 1D, Supplementary Table 4), corroborating the previous results obtained by manual grading. Next, centrosomes were divided into thirds by their NeonGreen to total signal ratio, with the highest, middle, and lowest thirds being labelled “green”, “yellow” and “orange” respectively. Again, we found increased orange centrosomes in the VZ and more green centrosomes in the non-ventricle areas within organoids (Supplementary Figure 1E-F, Supplementary Table 5). Taken together, these data indicate that the older, tdTomato-enriched centrosomes are preferentially retained by VZ NPCs, whereas the differentiating progeny inherits the younger, more NeonGreen-containing centrosomes.

Ninein knockdown affects NPC fate

Next, we wanted to understand how centrosome inheritance affects the behaviour of human NPCs. Previous work identified that a knockdown of Ninein can randomise inheritance by preventing centriole maturation, without impeding the cells’ ability to divide (Wang et al., 2009). We produced constructs that expressed human Ninein targeting shRNA or a scrambled shRNA under the U6 promoter, as well as an H2B-CFP to facilitate identification of targeted cells (Supplementary Figure 2A). To test the efficacy of the shRNA, we transfected HEK cells with the constructs and stained them for Ninein as well as centrosomal marker Pericentrin (Supplementary Figure 2C, Supplementary Table 6). Analysis of the intensity of the Ninein signal showed a significant decrease between scrambled and Ninein-targeting shRNAs (Supplementary Figure 2D). Ninein-targeting and control shRNA-expressing constructs were then electroporated into the VZ of day 35 WT human forebrain

organoids (Figure 3A). After 5 days, we assessed the cell types of shRNA- targeted cells by co-staining with SOX2 or CTIP2 (Figure 3B-D, Supplementary Table 2). Strikingly, we found a decrease in the proportion of SOX2-positive cells upon Ninein knockdown, which corresponded with a significant increase in the neuronal, CTIP2-positive population. These data suggest that knockdown of Ninein, and therefore possibly randomization of centrosome inheritance, leads to precocious neuronal differentiation of NPCs in the ventricular zone (Figure 3B-D).

Ninein knockdown alters centrosome segregation

As Ninein knockdown caused an increase in CTIP2-positive neurons, we next analyzed whether the older centrosome was still retained in the VZ or if it was also inherited by the differentiating daughter cell. To ensure constitutive expression of shRNA and recombination of only the cells expressing the shRNA, we generated constructs that expressed CRE-ER^{T2} and the shRNA (Supplementary Figure 2B) on a retroviral backbone. Day 24 organoids derived from Centriolin-RITE (CRE-ER^{T2} negative) hESCs were transduced with either scrambled or Ninein-targeting shRNA retroviruses (Figure 4A). Organoids were induced with 4-OH tamoxifen, fixed 22 days later and their centrosomes colours were manually analysed (Figure 4B). Remarkably, we observed a shift in the localisation of the old centrosomes in the Ninein knockdown condition as compared to the scrambled, with an increase in old (orange) and a decrease in young (green) non-ventricular centrosomes in the Ninein knockdown cells as compared to the scrambled condition (Figure 4C-D, Supplementary Table 3). This corresponded with the reverse seen in younger (green) centrosomes, where Ninein knockdown caused a substantial increase in green centrosomes in ventricular regions (Figure 4C-D). Taken together, these data

suggest that Ninein plays a role in the inheritance of the older centrosome in the cells of the VZ and that aberration of Ninein, here through shRNA mediated knockdown, leads to segregation of the older centrosome also into non-ventricular areas, associated with impaired NPC behaviour.

Discussion

We here identify asymmetric inheritance of the older and more mature centrosome by ventricular NPCs in a model of the developing human cortex, which has hitherto not been described in human tissues. Such non-random and preferential inheritance of one of the centrosomes depending on centrosomal age by one of the two daughter cells has previously been reported for asymmetric cell divisions in yeast, drosophila, and mice. The evolutionary conservation of this phenomenon emphasises the important role that centrosome inheritance may play in maintaining the proper cellular behaviour during asymmetric cell division.

The reason why human ventricular NPCs retain the older mother centrosome remains unclear. Several hypotheses may explain preferential inheritance of the old centrosome to the self-renewed daughter NPC. One potential reason could be that inheritance of the old centrosome may reduce aberrant mitotic events as the mother centrosome had participated previously in at least one successful mitosis, suggesting that the centrosome is capable of producing a daughter centriole, nucleating microtubules, and facilitating normal chromosome segregation, while the newly synthesized daughter centrosome is newer and less “tested” as it has never produced a functional centrosome. If this centrosome has an aberration in its structure, it could lead to duplication defects and deleterious chromosomal missegregation. Thus, one may hypothesize that evolution would favour retaining the older, tested centrosome with the daughter cell that must undergo additional rounds of cell divisions. In support of this notion, the older centrosome is inherited by self-renewing NPCs in mouse (Wang et al., 2009) and, as we here show, in human cortical development, and by the daughter cell in budding yeast (Pereira et al., 2001;

Lengefeld et al., 2017), which is considered the stem cell. In contrast, drosophila neuroblasts inherit the younger centrosome and pass on the older centrosome to their differentiating daughter cells (Januschke et al., 2011). Why drosophila neuroblasts do not follow the mode of centrosome inheritance observed in other species is not known. One may speculate that drosophila neuroblasts produce less progeny and therefore have lower selective pressure to maintain their fitness.

Another potential reason for asymmetric inheritance could be that the old centrosome of NPCs is maintained on the ventricular wall associated with the primary cilium. Indeed, it has been shown that the mother centrosome is quicker to reassemble the primary cilium, likely because it was already decorated with the distal appendages from the previous interphase (Paridaen et al., 2013), which has been shown to be critical for NPC cellular behaviour. Moreover, at the ventricular wall, space is limited, and the apical feet of ventricular NPCs are crowded together forming adherens junctions. The stability of these junctions and the maintenance of the apical foot itself is dependent on the junctional microtubules (Kasioulis et al., 2017), which can be destabilised by increased centrosomal microtubule organisational activity (Camargo Ortega et al., 2019). Indeed, previous work showed that overexpression of the centrosomal protein AKNA increased centrosomal microtubule organisational activity, destabilised the apical junction, and caused NPCs to delaminate from the apical surface and migrate out of the VZ. Furthermore, the mother centrosome was shown to anchor to the apical membrane via the distal appendage protein CEP83 (Shao et al., 2020). Loss of CEP83 causes impaired apical anchorage of the centrosome, disorganisation of microtubules, increase in NPC proliferation and subsequent enlargement of the cortex. These data indicate that the maintenance of NPCs in the ventricular zone requires a delicate balance of

316 centrosomal function at the apical surface. Inheritance of the older centrosome could
317 be one mechanism by which NPCs regulate this balance. Removing Ninein from the
318 centrosome could alter this balance and lead to the older centrosome being inherited
319 to a non-ventricle destined cell. Additionally, it is becoming apparent that
320 centrosomes act as one of the key signalling centres of the cell (Arquint et al., 2014).
321 The Notch signalling regulator, Mind-bomb1, was shown to be preferentially enriched
322 on the daughter centrosome and asymmetrically segregated with it into the
323 differentiating daughter cell (Tozer et al., 2017). Mind-bomb1 in this cell would then
324 promote stemness via Notch signalling activation in the surrounding NPCs.
325 Consistent retention of particular centrosome allows of such asymmetric signalling
326 pathways to be established and could facilitate the coordination of other cellular
327 asymmetries (Royall and Jessberger, 2021).

328 The extent to which proper asymmetric inheritance of the older centrosome by
329 dividing NPCs is associated with human disease remains currently unknown. For
330 example, disturbance of asymmetric inheritance of centrosomes could play a
331 causative role in microcephaly where indeed a substantial number of human variants
332 and mutations have been identified in genes associated with centrosome function
333 and structure (Faheem et al., 2015). Strikingly, a recent cell type-specific analysis of
334 centrosomal proteomes identified a large number of proteins, previously implicated
335 with neurodevelopmental disease, to be associated with centrosomes (O'Neill et al.,
336 2022). We here identify that human NPCs show asymmetric inheritance of
337 centrosomes and that disrupting retention of the pattern of centrosome inheritance
338 affects proper neurogenesis in human forebrain organoids. Together with these proof
339 of principle findings, the genetic approach we present here may become a powerful
340 tool in elucidating the role centrosome inheritance plays in human disease and

cortical malformations. Indeed, the Centriolin-RITE tool kit presents a number of benefits over the previously described photoconversion-based approach (Wang et al., 2009). Photoconversion requires the tagged proteins to be targeted with a laser, which requires surgery or tissue extraction to allow for laser accessibility. This potentially alters the natural physiological processes within the tissues and may introduce experimental artefacts. Furthermore, photoconversion inevitably produces phototoxic events in cells which may alter their behavior. The Centriolin-RITE birthdating tool can be activated in a spatial and temporal dependent manner by the use of tamoxifen-inducible Cre approaches. This allows any tissues within an organism to be birthdated without having to physically disturb it. Additionally, we designed the RITE system to use fluorescent proteins tdTomato and NeonGreen that originate from two evolutionary distinct species: *Discosoma sp.,* and *Branchiostoma lanceolatum,* respectively (Shaner et al., 2004; Shaner et al., 2013). This facilitates biochemical separation of the birthdated proteins by immunoprecipitation; further, the addition of high-affinity biochemical tags to the RITE cassette is feasible and will allow for further biochemical and proteomics-based analyses, which are essential to untangling the complex protein-protein interactions in centrosomes (O'Neill et al., 2022). The data we present here show that asymmetric inheritance of centrosomes is an evolutionary conserved mechanism during cortical formation that may be of critical relevance for human brain development by maintaining the proper cellular behaviour of human neural progenitor cells.

Methods

Genetic targeting and constructs

Guide RNAs and CRISPR/Cas9 tagging was performed as described previously (Denoth-Lippuner et al., 2021). ENSEMBL (www.ensembl.org) was used to find the full sequences of the gene of interest and the terminal stop codon. The Zhang group guide design tool (www.crispr.mit.edu) was used to find best gRNAs, based on the closeness to the stop codon and the lowest number of off-targets. Guides were synthesised from Microsynth AG, Switzerland and cloned into pSpCas9(BB)-2A-Puro (Addgene 48139) following the cloning strategy described by Ran *et al*. (Ran et al., 2013). The following gRNAs were used:

Human CNTRL: ACAAGACAGTATTCCTCATC

Human ER^{T2}-Cre-ER^{T2}: GGGGCCACTAGGGACAGGAT

To generate the homology arms required for the insertion of the construct via homologous-directed repair, an upstream and downstream region immediately adjacent to the terminal stop codon of the gene of interest was PCR amplified. Primers used were:

Human CNTRL

Upstream homology Forward: GCCTCTTTAATGTGCCCAAG

Upstream homology Reverse: TCTGGCTGAGGCATTCTTTTC

Downstream homology Forward: TGAGGAATACTGTCTTGTGTAAATATATTC

Downstream homology Reverse: CTTGGTGGTGAGGGATGACT

Upon establishment of a cell line, genomic DNA was extracted using Qiagen DNeasy Blood & Tissue Kit (Qiagen 69504). Primers to test correct integration of the construct were designed such a way that one primer was within the inserted, non-native DNA and one was outside the inserted DNA including the homology arms. Additional primers were designed that would span the whole inserted region; these would test for homozygous vs heterozygous integration. PCRs were performed on WT and genetically modified genome DNA. CAG-Cre (Addgene No 13776) was used for recombination via electroporation. AAVS1-T2A-Puro_CAG-ER^{T2}-Cre-ER^{T2}was cloned by replacing DR-GFP from pAAVS1-DR-GFP (Addgene No 113193) with ER^{T2}-Cre-ER^{T2}fragment was obtained from CAG-ER^{T2}-Cre-ER^{T2} (addgene 13777) via restriction digest. shRNAs were taken from broad institute database (www.portals.broadinstitute.org/gpp/public/gene/search) and cloned into a retroviral backbone; viruses were produced as described before (Bin Imtiaz et al., 2021). Later, H2B-CFP was removed from the constructs and replaced with CRE-ER^{T2} that was taken from CAG-ER^{T2}-Cre-ER^{T2}(Addgene 13777).

Human ESCs and organoids

All hESC experiments were approved by the Kantonale Ethik-Kommission (KEK) of the canton of Zurich, Switzerland. H9 hESCs were maintained in feeder-free conditions and grown at 37°C with 5% CO_2 (Thomson et al., 1998). hESCs were fed with mTeSR1 or mTeSR plus (Stem Cell Technologies) in the absence of antibiotics and grown on hESC qualified Matrigel (Corning) coated plates. ReLeSR (Stem Cell Technologies) was used for routine passaging as it promotes stemness. Passaged cells were kept in media containing 10μM Y-27632 (Stem Cell Technologies) for 24 hours to promote survival. Some protocols required a single cell suspension of

hESCs (e.g., electroporations, aggrewells); to obtain a single cell suspension, hESCs were instead passaged with Accutase (Sigma-Aldrich). For freezing down, hESCs were resuspended in CryoStore CS10 (Sigma-Aldrich) and stored below -170°C in liquid nitrogen. For electroporations, hESC were maintained in media containing Y-27632 for at least 1 hour to improve cell survival. Approximately two million cells were used per electroporation. Chilled Nucleofector V (Lonza) was used as the electroporation medium, and the electroporation was performed on the AMAXA electroporation system using the programme A-23. For overexpression, 1µg of DNA per plasmid was electroporated. For gene editing, 4µg of DNA per plasmid was electroporated. Recombination of Cre-ER^{T2}expressing cells was induced in ER^{T2}-Cre-ER^{T2} expressing cells by administration of 0.5µM 4-hydroxytamoxifen (Sigma-Aldrich) for 24 hours. Neomycin resistant cells were selected with 100µg/ml G418 sulfate (Gibco). Puromycin resistant cells were selected with 1µg/ml puromycin (Gibco).

The human forebrain organoid protocol was described before (Qian et al., 2016; Qian et al., 2018). We used a modified form of this protocol, and the adjustments are as follows.

Day 0, maintenance of hESC and EB formation. hESCs were cultured in feeder free conditions. To produce EBs on day 0 a single cell suspension was acquired with the use of Accutase. hESCs were incubated with 10µM Y-27632 at least 1 hour prior to passaging to promote survival. The number of cells in the suspension was estimated with use of a cytometer and appropriate volume of suspension was added to AggreWell 800 (Stem Cell Technologies) that would result in 5000 cells per microwell being produced. AggreWells were pre-treated with Anti-adherence Rinsing

435 Solution (Stem Cell Technologies) and AggreWell plates were centrifuged following
436 the manufacturer's guidelines.

437 *Day 1-4, Harvesting EBs and maintenance of EBs*. On day 1 EBs are harvested
438 following the AggreWell manufacturer's guide by gently pipetting with either a 5ml
439 pipette or a 1ml pipette with the tip cut off. Prior to harvesting, medium was ran the
440 full length of the pipette to reduce the adherence of EBs to the side of the pipette.
441 EBs were transferred to a 6 well Ultra-Low Attachment Plate (Corning) or a 10cm
442 Ultra-Low Attachment Plate (Corning) and maintained in mTeSR-E5 (Stem Cell
443 Technologies) with 2μM Dorsomorphin (Sigma-Aldrich) and 2μM A83-01 (Tocris)
444 until day 4. Media was changed day 3 and 4.

445 *Day 5-14, Adaption and maintenance in Induction media*. Days 5 to 14 follow the
446 exact same steps as described in Qian et al. 2018, but with a different media. The
447 induction media used was mTeSR-E5 with 1μM CHIR99021 (Stem Cell
448 Technologies) and 1μM SB-431542 (Stem Cell Technologies).

449

450 *Imaging and immunostaining*

451 hESCs were fixed by either incubation with prewarmed 4% paraformaldehyde
452 (Sigma-Aldrich) for 15 minutes at room temperature or with chilled methanol (Sigma-
453 Aldrich) for 20 minutes at 4□. All monolayer immunostainings used 3% Donkey
454 Serum (Millipore) as a blocking agent and 0.25% Triton-X (Sigma-Aldrich) as a
455 permeabilization agent. Primary antibodies were incubated with the samples at 4□
456 overnight and secondary antibodies were incubated for 1 hour and 30 minutes at
457 room temperature. Zeiss LSM 800 confocal microscope was used to obtain all
458 images. For live cell imaging, hESCs were maintained at 37□ and with 5% CO2

facilitated by the incubator chamber and heated stage that is fitted to the microscope. hESCs were imaged in Matrigel coated Lab Tek II chambered cover glasses (Thermo Fisher Scientific). For imaging following electroporation, cells were plated on the Lab Tek cover glasses. Imaging started after at least 6 hours. For imaging involving ER^{T2}-Cre-ER^{T2}expressing cells, hESCs were first plated on Lab Tek chambered coverglasses (Thermos Fisher Scientific) and allowed to settle for at least 24 hours. Recombination was induced *in situ* with the addition of 0.5μM 4-hydroxytamoxifen (Sigma-Aldrich) into the media. hESCs were imaged every hour. Throughout imaging hESCs were maintained in mTeSR plus containing 10μM Y-27632 and Penicillin-Streptomycin-Amphotericin B (Anti-Anti, Thermo Fisher Scientific). Additionally, media was supplemented with 1:1000 SiR-DNA (Spirochrome), in the absence of Verapamil, to visualise the nucleus and facilitate easier tracking of cells. Media was changed every 24 hours.

Organoids were electroporated as described (Denoth-Lippuner et al., 2021; Denoth-Lippuner et al., 2022). Recombination was induced in ER^{T2}-Cre-ER^{T2}expressing organoids by administration of 10μM 4-hydroxytamoxifen (Sigma-Aldrich) for 48 hours. Organoids were fixed with prewarmed 4% paraformaldehyde (Sigma-Aldrich) for 15 minutes at room temperature. Fixed organoids were suspended in 30% sucrose overnight at 4 °C; organoids were maintained in 30% sucrose until sectioned. For sectioning, organoids were embedded in OCT compound (Tissue-Tek) and frozen solid. 20-40μm sections were sectioned using a cryostat and adhered to cover slides. Sections were kept at -20°C until stained. For tissues containing fluorophores, proper measures were undertaken to prevent unnecessary and extensive exposure to light during the whole process. All organoid immunostainings used 10% Donkey Serum (Millipore) as a blocking agent and 0.5%

Triton-X (Sigma-Aldrich) as a permeabilization agent. Primary antibodies were incubated with the samples at 4°C for 1-3 nights and secondary antibodies were incubated for 1 hour and 30 minutes at room temperature. The signal of H2B-CFP electroporated organoids was amplified using an anti-GFP antibody.

Image analysis

All images were analysed using ImageJ/Fiji and the data was processed and analysed in Excel or R. For organoid analysis, images with ventricular recombined centrosomes were selected. The thickness of the ventricle was measured using the SOX2 staining as the outer boundary. A circle with a radius of a maximum of 3 times the ventricle thickness or to the edge of the tissue (which ever was less), centred on the ventricle midpoint was cropped out. The centre of the ventricle was cropped out leaving a ring of 3-5 centrosomes, care was taken not to crop out recombined centrosomes that were part of the same cluster. A line was drawn between the two ends of the cluster. A perpendicular line was draw in the middle of the line extending radially out of the ventricular zone to the edge of the circle. Two more lines were drawn from the ends of the first line at an angle of 45° extending to the edge of the circle. The area within these 3 lines and the arc of the edge of the circle was cropped out and analysed.

Recombined centrosomes were manually assigned one of three colours, orange, yellow or green. The criteria for each were as follows and were dependent on the unrecombined centrosomes in the same image. Orange centrosomes were centrosomes with both tdTomato and NeonGreen signal, and where the tdTomato signal was similar to that of unrecombined centrosomes. Yellow centrosomes had

both tdTomato and NeonGreen signal, but the tdTomato signal was visibly less than unrecombined centrosomes. Green centrosomes had only NeonGreen signal; the tdTomato signal in these centrosomes was undetectable by eye. The ventricular centrosomes (vent) and non-ventricular centrosomes (nonvent) were counted by colour for each image. Ratios of each colour were calculated and compared between different images. The absolute counts of centrosomes by colour were calculated across images and compared by their region. Additionally, the ratio of counts between regions was calculated for each colour.

Centrosomes were analysed in two groups: centrosomes from the ventricle (vent) and centrosomes outside the ventricle (nonvent). Vent centrosomes were defined as the centrosomes visibly localised on the ventricular wall, identifiable by the high density of centrosomes in a circular configuration. Nonvent centrosomes were centrosomes localised outside of the ventricular wall. Centrosomes were drawn around and the mean signal intensity was recorded for tdTomato and NeonGreen. The ratio of NeonGreen to total signal was calculated by dividing the NeonGreen by the sum of tdTomato and NeonGreen signal. Means of this ratio were calculate for each region of each image. This ratio was used for the digital allocation of orange, yellow and green, with the centrosomes in the top third for highest ratio being assigned green, the second third yellow and the lowest ratio centrosomes being assigned orange.

Used antibodies:

Antibody	Species	Manufacturer	Catalogue No. / RRID	Dilution
PCNT	Rabbit	Abcam	ab4448 RRID:AB_304461	1:1000

SOX2	Rabbit	Millipore	AB5603 RRID:AB_2286686	1:200
SOX2	Mouse	R&D	MAB2018 RRID:AB_358009	1:200
CTIP2	Rat	Abcam	ab18465 RRID:AB_2064130	1:200
CEP164	Rabbit	Abcam	ab221447 / n.a.	1:200
tdTomato	Goat	Origene	AB8181-200 / n.a.	1:750
Ninein	Mouse	Santa Cruz	sc-376420 RRID:AB_11151570	1:250
GFP	Chicken	Aves	GFP.1020 RRID:AB_10000240	1:1000

Statistical analysis

Statistical significance of all data presented here was tested by using unpaired, students T-test. Significance is represented with asterisks and ns, which correspond to the following p values: ns = $p > 0.05$, * = $p < 0.05$, ** = $p < 0.01$, *** = $p < 0.001$. The number of analysed data for the control and the test condition were kept the same. The number of analysed data represented in the figure legend as n, where n is equal to the number of control or test data points.

Funding Information

This work was supported by the European Research Council (STEMBAR to S.J.), the Swiss National Science Foundation (BSCGI0_157859 and 310030_196869 to S.J.), the Boehringer Ingelheim Fonds (to L.N.R), and the Zurich Neuroscience Center. Fundings sources were not involved in study design, data collection and interpretation, or decision to submit the work for publication.

Acknowledgements

We thank Y. Barral for critical conceptual input.

Declaration of interests

The authors declare no competing interests.

References

Arquint C, Gabryjonczyk A-M, Nigg EA (2014) Centrosomes as signalling centres. Philosophical transactions of the Royal Society of London Series B, Biological sciences 369.

Bin Imtiaz MK, Jaeger BN, Bottes S, Machado RAC, Vidmar M, Moore DL, Jessberger S (2021) Declining lamin B1 expression mediates age-dependent decreases of hippocampal stem cell activity. Cell Stem Cell.

Bornens M (2002) Centrosome composition and microtubule anchoring mechanisms. Current opinion in cell biology 14:25-34.

Cadwell CR, Bhaduri A, Mostajo-Radji MA, Keefe MG, Nowakowski TJ (2019) Development and Arealization of the Cerebral Cortex. Neuron 103:980-1004.

Camargo Ortega G et al. (2019) The centrosome protein AKNA regulates neurogenesis via microtubule organization. Nature 567:113-117.

Chong WM, Wang W-J, Lo C-H, Chiu T-Y, Chang T-J, Liu Y-P, Tanos B, Mazo G, Tsou M-FB, Jane W-N, Yang TT, Liao J-C (2020) Super-resolution microscopy reveals coupling between mammalian centriole subdistal appendages and distal appendages. Elife 9.

Denoth-Lippuner A, Royall LN, Gonzalez-Bohorquez D, Machado D, Jessberger S (2022) Injection and electroporation of plasmid DNA into human cortical organoids. STAR Protocols 3:101129.

Denoth-Lippuner A, Jaeger BN, Liang T, Royall LN, Chie SE, Buthey K, Machado D, Korobeynyk VI, Kruse M, Munz CM, Gerbaulet A, Simons BD, Jessberger S (2021) Visualization of individual cell division history in complex tissues using iCOUNT. Cell Stem Cell 28:2020-2034 e2012.

Di Lullo E, Kriegstein AR (2017) The use of brain organoids to investigate neural development and disease. Nature reviews 18:573-584.

Faheem M, Naseer MI, Rasool M, Chaudhary AG, Kumosani TA, Ilyas AM, Pushparaj P, Ahmed F, Algahtani HA, Al-Qahtani MH, Saleh Jamal H (2015) Molecular genetics of human primary microcephaly: an overview. BMC medical genomics 8 Suppl 1:S4.

Gao P, Postiglione MP, Krieger TG, Hernandez L, Wang C, Han Z, Streicher C, Papusheva E, Insolera R, Chugh K, Kodish O, Huang K, Simons BD, Luo L,

582 Hippenmeyer S, Shi SH (2014) Deterministic progenitor behavior and unitary
583 production of neurons in the neocortex. Cell 159:775-788.
584 Gromley A, Jurczyk A, Sillibourne J, Halilovic E, Mogensen M, Groisman I, Blomberg
585 M, Doxsey S (2003) A novel human protein of the maternal centriole is
586 required for the final stages of cytokinesis and entry into S phase. The Journal
587 of cell biology 161:535-545.
588 Gromley A, Yeaman C, Rosa J, Redick S, Chen C-T, Mirabelle S, Guha M,
589 Sillibourne J, Doxsey SJ (2005) Centriolin anchoring of exocyst and SNARE
590 complexes at the midbody is required for secretory-vesicle-mediated
591 abscission. Cell 123:75-87.
592 Hansen DV, Lui JH, Parker PR, Kriegstein AR (2010) Neurogenic radial glia in the
593 outer subventricular zone of human neocortex. Nature 464:554-561.
594 Hotz M, Leisner C, Chen D, Manatschal C, Wegleiter T, Ouellet J, Lindstrom D,
595 Gottschling DE, Vogel J, Barral Y (2012) Spindle pole bodies exploit the
596 mitotic exit network in metaphase to drive their age-dependent segregation.
597 Cell 148:958-972.
598 Januschke J, Llamazares S, Reina J, Gonzalez C (2011) Drosophila neuroblasts
599 retain the daughter centrosome. Nat Commun 2:243.
600 Kashihara H, Chiba S, Kanno Si, Suzuki K, Yano T, Tsukita S (2019) Cep128
601 associates with Odf2 to form the subdistal appendage of the centriole. Genes
602 to Cells 24:231-243.
603 Kasioulis I, Das RM, Storey KG (2017) Inter-dependent apical microtubule and actin
604 dynamics orchestrate centrosome retention and neuronal delamination. Elife 6.
605 Lancaster MA, Renner M, Martin CA, Wenzel D, Bicknell LS, Hurles ME, Homfray T,
606 Penninger JM, Jackson AP, Knoblich JA (2013) Cerebral organoids model
607 human brain development and microcephaly. Nature 501:373-379.
608 Lengefeld J, Hotz M, Rollins M, Baetz K, Barral Y (2017) Budding yeast Wee1
609 distinguishes spindle pole bodies to guide their pattern of age-dependent
610 segregation. Nature cell biology 19:941-951.
611 Libe-Philippot B, Vanderhaeghen P (2021) Cellular and Molecular Mechanisms
612 Linking Human Cortical Development and Evolution. Annu Rev Genet 55:555-
613 581.
614 Llinares-Benadero C, Borrell V (2019) Deconstructing cortical folding: genetic,
615 cellular and mechanical determinants. Nature reviews 20:161-176.

Noctor SC, Martinez-Cerdeno V, Ivic L, Kriegstein AR (2004) Cortical neurons arise in symmetric and asymmetric division zones and migrate through specific phases. Nat Neurosci 7:136-144.

O'Neill AC et al. (2022) Spatial centrosome proteome of human neural cells uncovers disease-relevant heterogeneity. Science (New York, NY 376:eabf9088.

Ostrem B, Di Lullo E, Kriegstein A (2017) oRGs and mitotic somal translocation - a role in development and disease. Current opinion in neurobiology 42:61-67.

Paridaen JTML, Wilsch-Bräuninger M, Huttner WB (2013) Asymmetric Inheritance of Centrosome-Associated Primary Cilium Membrane Directs Ciliogenesis after Cell Division. Cell 155:333-344.

Pereira G, Tanaka TU, Nasmyth K, Schiebel E (2001) Modes of spindle pole body inheritance and segregation of the Bfa1p-Bub2p checkpoint protein complex. The EMBO journal 20:6359-6370.

Qian X, Jacob F, Song MM, Nguyen HN, Song H, Ming GL (2018) Generation of human brain region-specific organoids using a miniaturized spinning bioreactor. Nature protocols 13:565-580.

Qian X et al. (2016) Brain-Region-Specific Organoids Using Mini-bioreactors for Modeling ZIKV Exposure. Cell 165:1238-1254.

Ran FA, Hsu PD, Wright J, Agarwala V, Scott DA, Zhang F (2013) Genome engineering using the CRISPR-Cas9 system. Nature protocols 8:2281-2308.

Ranjan R, Snedeker J, Chen X (2019) Asymmetric Centromeres Differentially Coordinate with Mitotic Machinery to Ensure Biased Sister Chromatid Segregation in Germline Stem Cells. Cell Stem Cell 25:666-681 e665.

Roemer EJ, West, Kesley L., Northrup, Jessica B., Iverson, Jana, M. (2016) 乳鼠心肌提取 HHS Public Access. Physiology & behavior 176:139-148.

Royall LN, Jessberger S (2021) How stem cells remember their past. Current opinion in cell biology 69:17-22.

Shaner NC, Campbell RE, Steinbach PA, Giepmans BNG, Palmer AE, Tsien RY (2004) Improved monomeric red, orange and yellow fluorescent proteins derived from Discosoma sp. red fluorescent protein. Nature biotechnology 22:1567-1572.

Shaner NC, Lambert GG, Chammas A, Ni Y, Cranfill PJ, Baird MA, Sell BR, Allen JR, Day RN, Israelsson M, Davidson MW, Wang J (2013) A bright monomeric green fluorescent protein derived from Branchiostoma lanceolatum. Nature methods 10:407-409.

Shao W, Yang J, He M, Yu X-Y, Lee CH, Yang Z, Joyner AL, Anderson KV, Zhang J, Tsou M-FB, Shi H, Shi S-H (2020) Centrosome anchoring regulates progenitor properties and cortical formation. Nature 580:106-112.

Sunchu B, Cabernard C (2020) Principles and mechanisms of asymmetric cell division. Development (Cambridge, England) 147.

Thomson JA, Itskovitz-Eldor J, Shapiro SS, Waknitz MA, Swiergiel JJ, Marshall VS, Jones JM (1998) Embryonic stem cell lines derived from human blastocysts. Science (New York, NY 282:1145-1147.

Tozer S, Baek C, Fischer E, Goiame R, Morin X (2017) Differential Routing of Mindbomb1 via Centriolar Satellites Regulates Asymmetric Divisions of Neural Progenitors. Neuron 93:542-551.e544.

Wang X, Tsai JW, Imai JH, Lian WN, Vallee RB, Shi SH (2009) Asymmetric centrosome inheritance maintains neural progenitors in the neocortex. Nature 461:947-955.

Figures

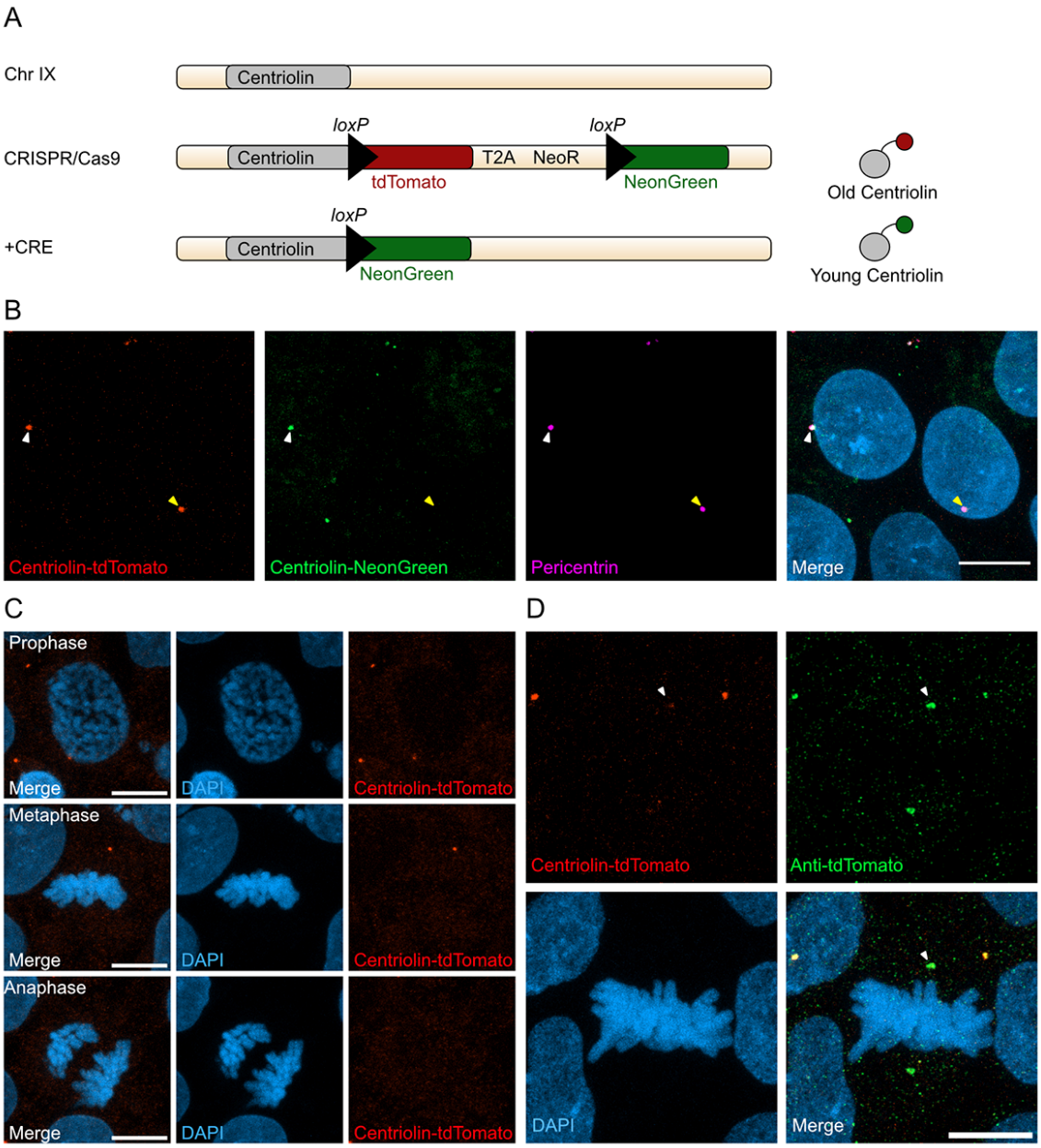

Figure 1. RITE-based birthdating of centrosomes. (A) Centriolin is tagged with the RITE system in hESCs so that all Centriolin protein made is tdTomato-tagged. Upon recombination with Cre recombinase, the tdTomato fluorophore is replaced with NeonGreen, making all new Centriolin protein tagged with NeonGreen. Identifying a proteins tag will indicate the proteins age with tdTomato being the oldest, then

675 NeonGreen. (B) Image of hESCs expressing Centriolin-RITE 24h post Cre induction.
676 Arrowheads point to Pericentrin-positive centrosomes where the Centriolin protein
677 localises to. The yellow arrowhead shows a centrosome that has not recombined,
678 whereas one depicted by the white arrowhead has recombined as indicated by the
679 appearance of NeonGreen signal. Scale bars, 10μm (C) Signal of Centriolin through
680 mitosis. In prophase centriolin signal is present, however the signal disappears in
681 metaphase and anaphase. Scale bars, 10μm (D) Staining for tdTomato protein
682 shows that Centriolin-tdTomato is present at the centrosome during metaphase but
683 that the signal is subsequently quenched. Scale bars, 10μm.

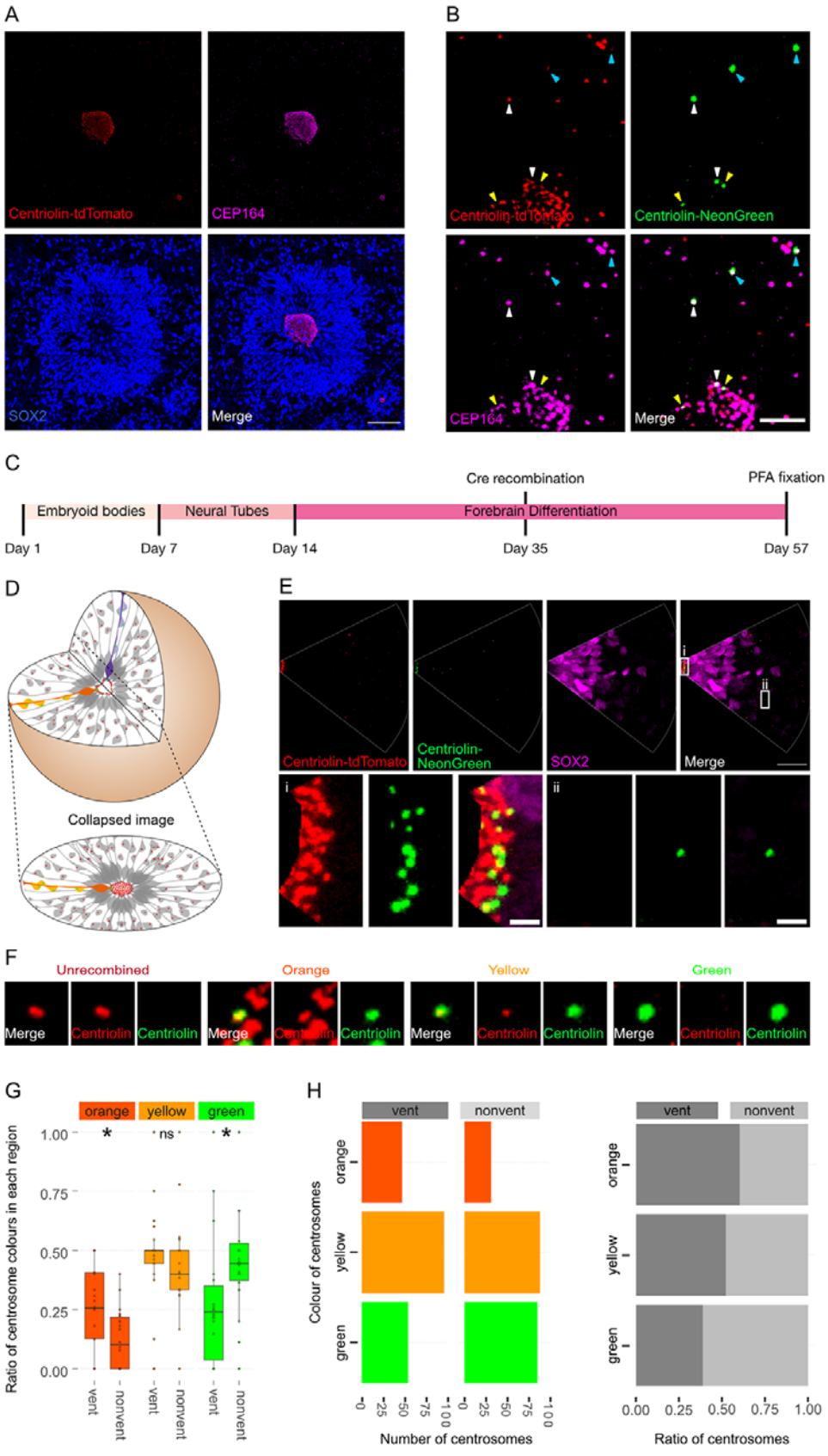

684

685 **Figure 2.** Asymmetric inheritance of centrosomes in human forebrain organoids. (A)
686 Cortical unit of a day 35 forebrain organoid. The ventricular zone is easily identified
687 by densly packed SOX2-positive NPCs that form a rosette-like structure around the
688 ventricular centrosomes, shown by Centriolin-tdTomato and the mother centriole
689 marker CEP164. Scale bar, 50μm. (B) Recombined centrosomes exhibiting variable
690 quantities of the older, Centriolin-tdTomato protein. Arrowheads indicate recombined
691 centrosomes identifiable by the presence of Centriolin-NeonGreen. White
692 arrowheads show centrosomes that have a large quantity of Centriolin-tdTomato
693 present, thus are the oldest. Blue arrowhead indicated centrosomes have visibly less
694 Centriolin-tdTomato, and the yellow arrowhead-depicted have no visible tdTomato
695 signal, suggesting these are the most recently formed centrosomes. Scale bar, 5μm.
696 (C) Scheme showing the timing of Cre recombination in the context of the organoid
697 protocol. (D) Schematic showing how imaging organoid sections causes the loss of
698 progeny of some NPCs. In this example, two NPCs have recombined (orange and
699 purple) and have produced progeny of a similar colour that migrate away along their
700 radial processes. When imaging sections that include a ventricle, both the orange
701 and purple NPCs' centrosomes are included in the image. The orange progeny are
702 also included because they migrate away along the x/y axis of the image. However,
703 as the purple NPCs' progeny will migrate away along the z-axis, they are not imaged.
704 (E) Example of an analysed image. The ventricular centrosomes are shown in large
705 in (i) and an example of non-ventricular centrosome is shown in (ii). Scale bars,
706 upper panel 20μm, (i - ii) 2μm. (F) Representative images that display the criteria of
707 manual colour allocation. Recombined centrosomes signal was compared to
708 unrecombined centrosomes. Centrosomes whose tdTomato signal was
709 indistinguishable from unrecombined were allocated orange, those that had less

tdTomato than unrecombined were yellow and those that had no tdTomato signal were green. Due to the presence of tdTomato signal, orange centrosomes would be the oldest, yellow the second oldest and green the youngest. (G-H) Analysis of the manual colour calling shows a significant enrichment of orange centrosomes in ventricle and a significant enrichment of green centrosomes outside of the ventricle (n = 22, cortical units). ns, non-significant, *$p < 0.05$

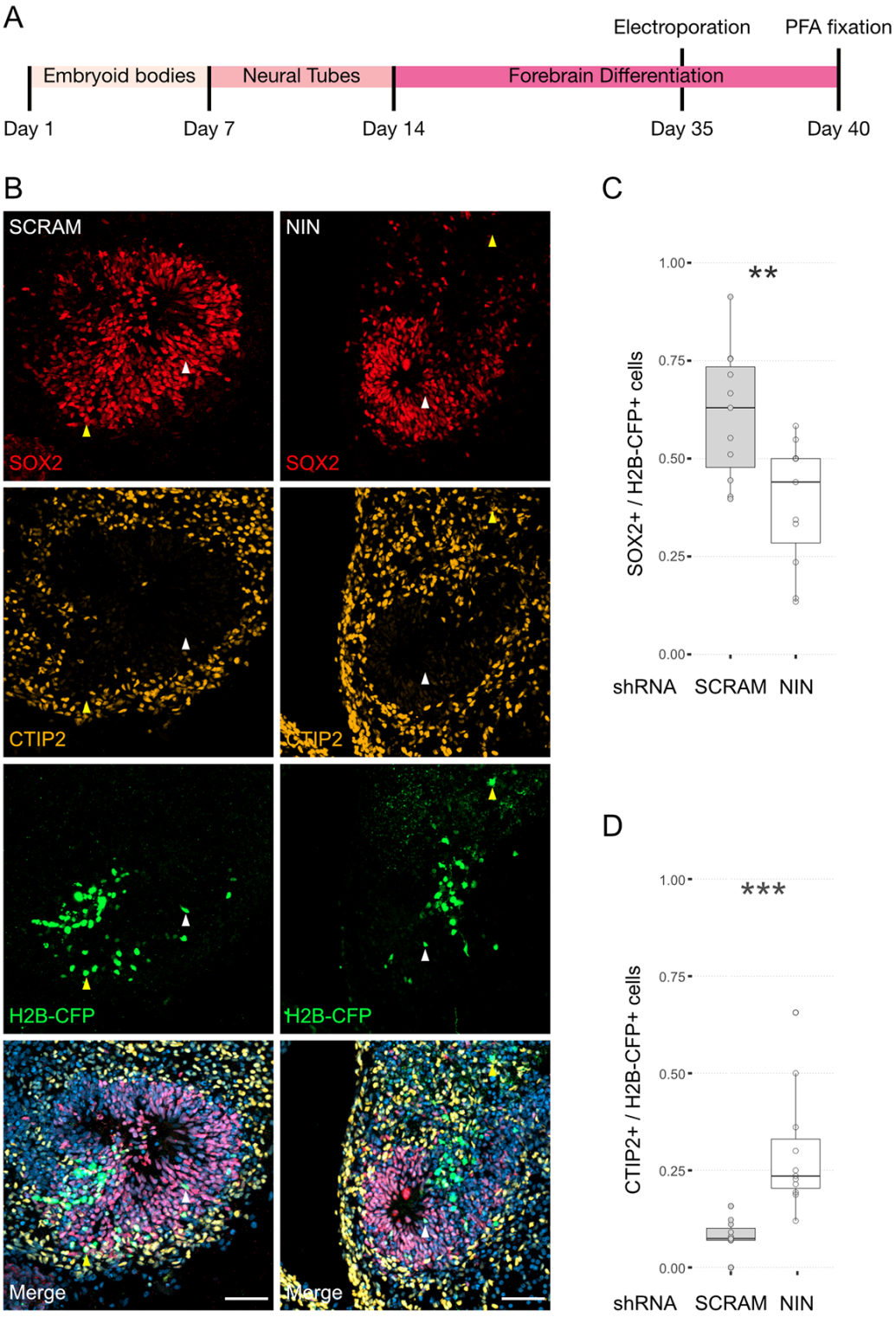

716

717 **Figure 3.** Randomisation of centrosome inheritance affects NPC fate. (A) Scheme

718 showing the timing of electroporation of the shRNA construct in the context of the

719 organoid protocol. (B) Day 40 WT organoids, 5 days post electroporation with either
720 scrambled shRNA or NIN-targeting shRNA, and a H2B-CFP marker. Scale bars,
721 50μm. (C) Graph of the ratio of SOX2-positive nuclei to H2B-CFP nuclei (n = 11,
722 cortical units). (D) Graph of the ratio of CTIP2-positive nuclei to H2B-CFP nuclei (n =
723 11, cortical units). $^{**}p < 0.01$, $^{***}p < 0.001$

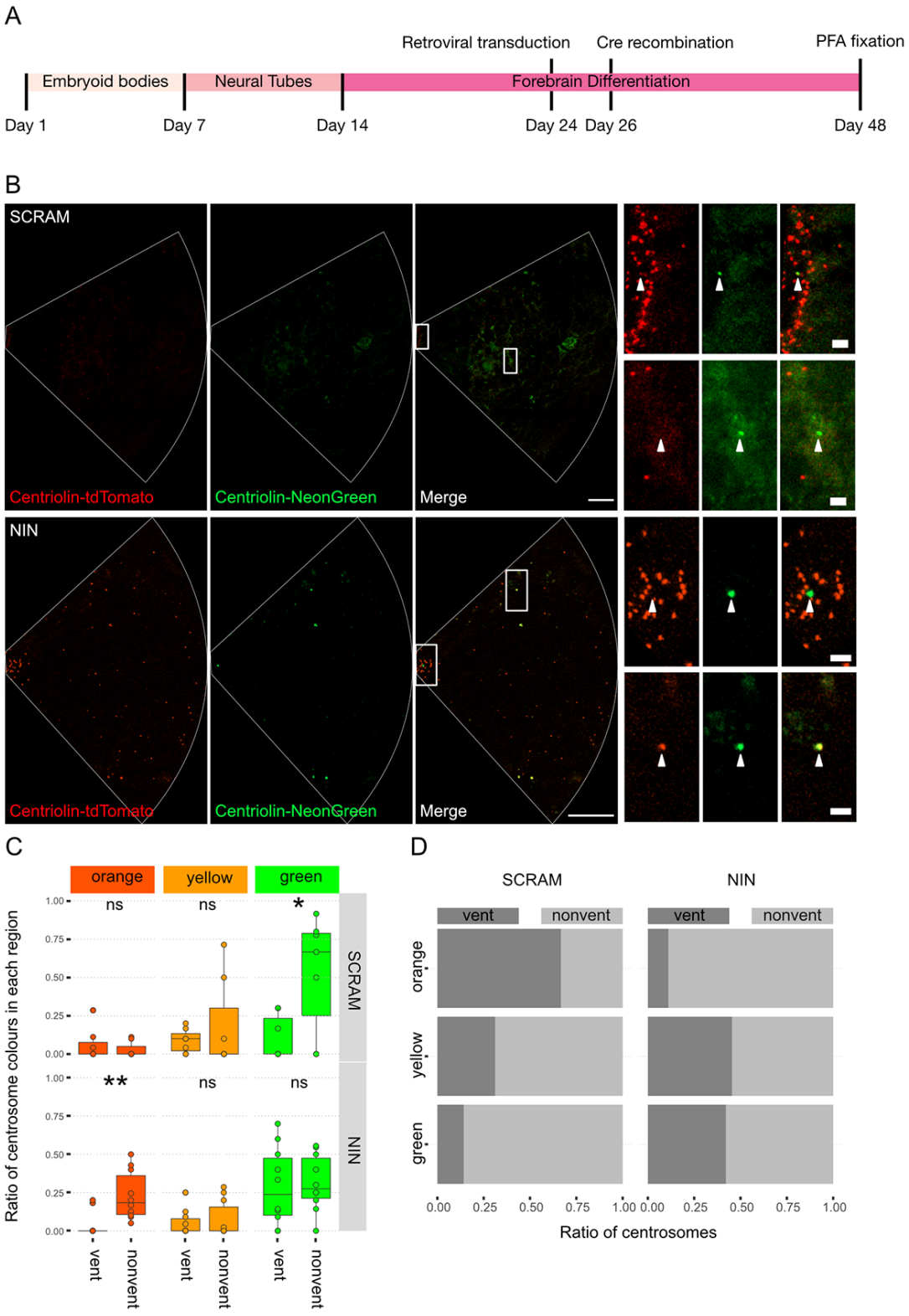

724

725 **Figure 4.** Ninein-shRNA alters retention of the older centrosome in the ventricular

726 zone. (A) Timing of the retroviral transduction and subsequent recombination in the

context of the organoid protocol. (B) Day 24 Centriolin-RITE organoids were infected with retroviral expression of scrambled or NIN-targeting shRNA, and Cre-ERT2. Organoids were fixed 22 days after recombination was induced with tamoxifen. Scale bars, 25μm (left column), 2μm (right column). (C) Comparison of the colour of centrosomes in each region by shRNA treatment using manual colour calling (scram n = 7, nin = 10 N, cortical units; note that single unit data overlay for “vent” data points). (D) Analysis of the colour composition of each region shows a shift in localisation of the older centrosomes to the nonvent region for the NIN shRNA treated organoids (n = 8, cortical units). ns, non-significant, *$p < 0.05$, **$p < 0.01$

Supplementary figures

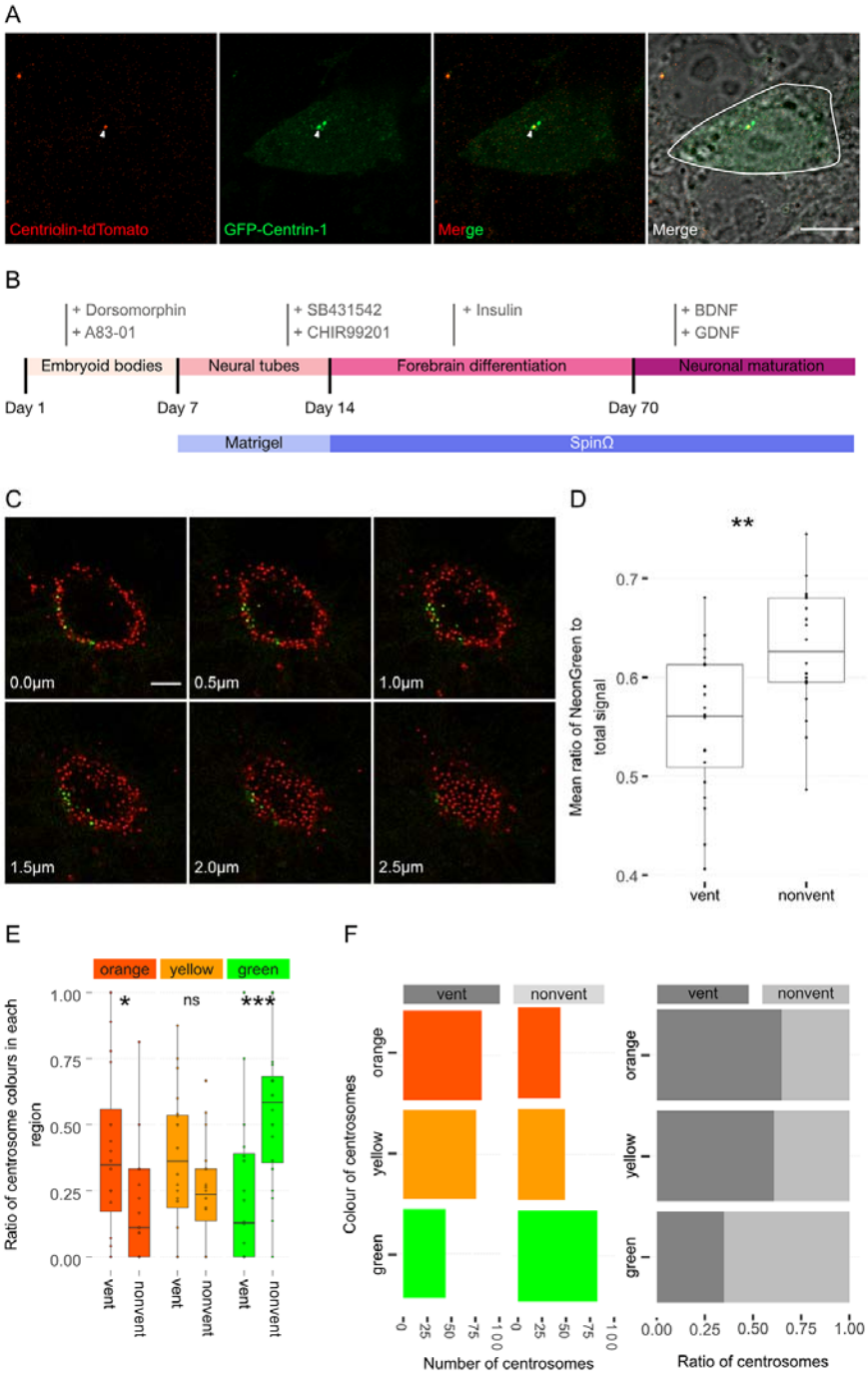

Supplementary Figure 1. Centrosome analyses in organoids. (A) hESC electroporated with GFP-Centrin-1 is outlined in white. Centriolin localises to only one of the two centrioles marked by GFP-Centrin-1. Scale bars, 10µm. (B) Scheme

742 showing a timeline of forebrain organoid protocol, with the small molecules used
743 during each part of the protocol. (C) Cross-sections of a ventricle show its 3-
744 dimensional, tubular/ spherical structure. Centrosomes are identified by their
745 endogenous Centriolin-tdTomato/Centriolin-NeonGreen signal. (D) Boxplot of mean
746 ratio of NeonGreen to total signal for each region, shows non-ventricular
747 centrosomes are significantly greener than the ventricular centrosomes (n = 20,
748 cortical units). (E-F) Automated colour calling from the ratio of NeonGreen to total
749 signal, this supports the manual data showing a significant enrichment of old
750 centrosomes in the ventricle (n = 20, cortical units). ns, non-significant, *$p < 0.05$, **p
751 < 0.01, ***$p < 0.001$

752

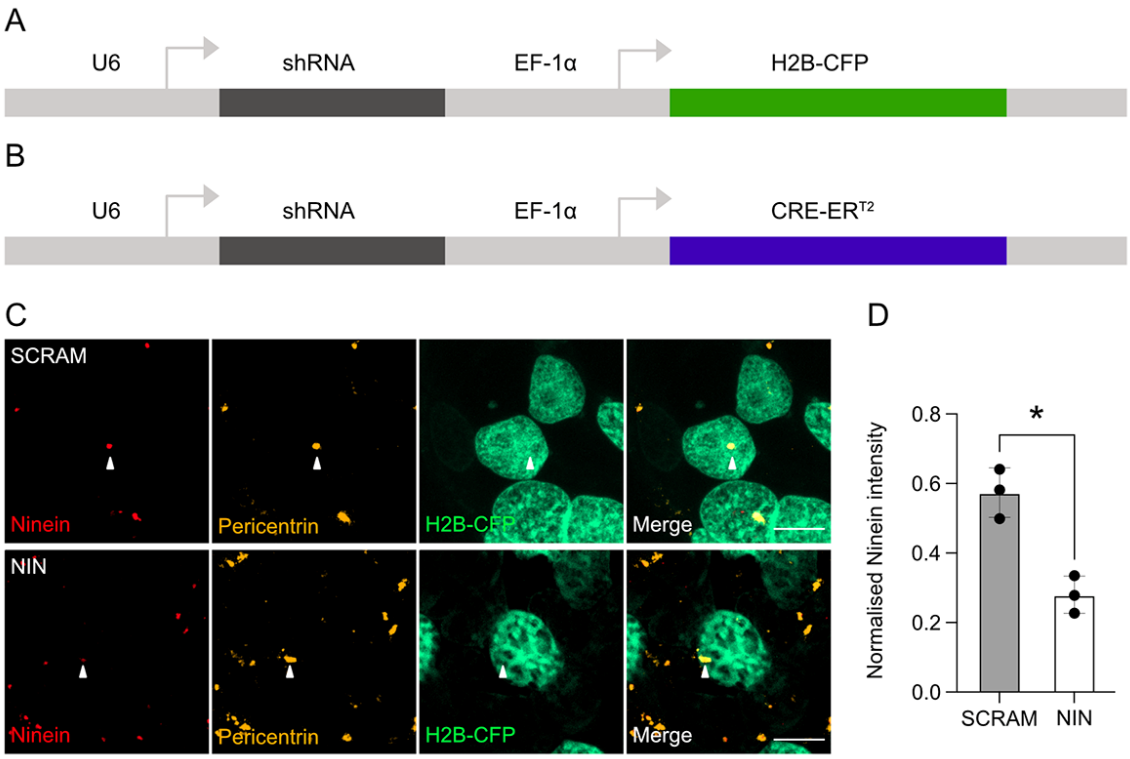

Supplementary Figure 2. Ninein knockdown in human cells. (A) Genetic map of the constructs used for the electroporation experiments. shRNA is expressed through the U6 promoter and the H2B-CFP is expressed via the EF-1α promoter. (B) Genetic map of the construct used for the generation of retroviruses. shRNA is expressed through the U6 promoter and the CRE-ER^{T2} is expressed via the EF-1α promoter. (C) Example images of the effect of transfection of the shRNAs targeting Ninein (NIN KD) and control shRNA (SCRAM) on Ninein expression in HEK cells. Scale bars, 10μm. (D) Graph of the mean Ninein signal of each replicate, corrected for background and normalised to the maximum centrosome signal within each replicate (n = 3, replicates; each replicate consisting of 5 images). *$p < 0.05$